

# Tribological Behavior of Plasma Spray Coatings for Marine Diesel Engine Piston Ring and Cylinder Liner

Jong-Hyun Hwang, Myoung-Seoup Han, Dae-Young Kim, and Joong-Geun Youn

(Submitted January 5, 2005; in revised form September 6, 2005)

High-temperature wear characteristics between plasma spray coated piston rings and cylinder liners were investigated to find the optimum combination of coating materials using the disc-on-plate reciprocating wear test in dry conditions. The disc and plate represented the piston ring and the cylinder liner, respectively. Coating materials studied were  $\text{Cr}_2\text{O}_3$ -NiCr,  $\text{Cr}_2\text{O}_3$ -NiCr-Mo, and  $\text{Cr}_3\text{C}_2$ -NiCr-Mo. Plasma spray conditions for the coating materials were established adjusting stand-off distance to obtain a coating with a porosity content of ~5%. It was found that a dissimilar coating combination of  $\text{Cr}_2\text{O}_3$ -NiCr-Mo and  $\text{Cr}_3\text{C}_2$ -NiCr-Mo provided the best antiwear performance. The addition of molybdenum was found to be beneficial to improve the wear resistance of the coating. Hardness differences between mating surfaces were also important factors in determining the wear characteristics, so that it should be controlled below 300 in Vickers hardness under dry conditions. Adhesive wear accompanying with metal transfer was a dominant wear mechanism for dry conditions.

**Keywords** abrasive, adhesive, ASTM G133, CV cast iron, gray cast iron, plasma spray coating, solid lubricant

## 1. Introduction

Modern marine diesel engines are required to operate under higher combustion pressures and temperatures for more efficient performance and to use a low-grade fuel to reduce fuel cost, so that abnormal wear at the piston ring and/or at the cylinder liner becomes a prevalent problem (Ref 1, 2). New demands for environmental, economical, and high-efficient technology have gradually increased to demand higher anti-wear properties and higher scuffing resistance for each component to enhance its performance. Plasma spray coating is a powerful method in improving the wear resistance of each component (Ref 3-5). A  $\text{Cr}_3\text{C}_2$ -NiCr-Mo-coated piston ring was applied commercially. However, excessive wear of the coated piston ring itself and cylinder liner has been reported under certain circumstances. Several factors, such as a high-temperature corrosive atmosphere, invasion of foreign particles, and failure of lubrication contribute to excessive wear. A high-temperature corrosive atmosphere of sulfuric acid is generated from chemical reactions between sulfur from fuel and water vapor from the intake air for combustion. The foreign particles result from wear debris of the piston ring and cylinder liner body and from carbon deposition caused by incomplete combustion. Inadequate lubrication is caused by an insufficient supply of lubrication oil in the early stages of engine operation. To cope with these situations, both engine designer and maker try to prevent formation of a corrosive atmosphere by controlling the combustion circumstances by means of systematic re-

forms as well as developing a trustworthy protective coating that can both overcome these severe operation conditions and provide optimum engine durability. In materials engineering especially, it might be the first task to select a pertinent coating that promises to minimize the wear rate of both the piston ring and the cylinder liner at the same time. Various coating materials have been developed and applied for this purpose up to now; for instance,  $\text{Al}_2\text{O}_3$ ,  $\text{Zr}_2\text{O}_3$ ,  $\text{Cr}_2\text{O}_3$ , WC-Co, WC-Ni,  $\text{Cr}_3\text{C}_2$ -NiCr, Mo, etc. (Ref 6). Of these,  $\text{Cr}_2\text{O}_3$  and  $\text{Cr}_3\text{C}_2$ -NiCr coatings are most widely used for covering wear processes, such as dry sliding, abrasion, and galling due to its higher hardness (2300 HV) and good high-temperature wear and erosion resistance (up to 1000 °C), respectively, and Mo for scuffing resistance. These coating materials are applied as individual compounds or as composites according to the required properties. Some studies (Ref 7, 8) showed that better wear characteristics were obtained when composite-type rather than individual-type coatings were used. As mentioned above, an important factor to be considered in evaluating the tribological characteristics of a piston ring coating material is the wear amount that occurs on the cylinder liner counterpart. From this point of view, the effect of the coating material combination on the wear characteristics of piston ring and cylinder liner was studied with the reciprocating wear test to determine the optimum combination of piston ring and cylinder liner coatings. Prior to this, it is also very important to establish the optimum spraying condition, which can result in a sturdy spray coating

**Table 1** Characteristics of the coating powders used in this study

Kind	Chemical composition	Powder morphology	Particle size, $\mu\text{m}$
Ceramic	99.5 $\text{Cr}_2\text{O}_3$	Blocky	22-45
	80Ni-20Cr	Spheroid	11-53
Metal	Mo	Spheroid, agglomerated	45-90
	$\text{Cr}_3\text{C}_2$ -30NiCr	Agglomerated	45-106

Jong-Hyun Hwang, Myoung-Seoup Han, Dae-Young Kim, and Joong-Geun Youn, Materials Research Department, Hyundai Industrial Research Institute, Hyundai Heavy Industries Co. Ltd., 1 Cheonha-dong, Dong-gu, Ulsan, South Korea 682-792. Contact e-mail: jhgh@hhi.co.kr.

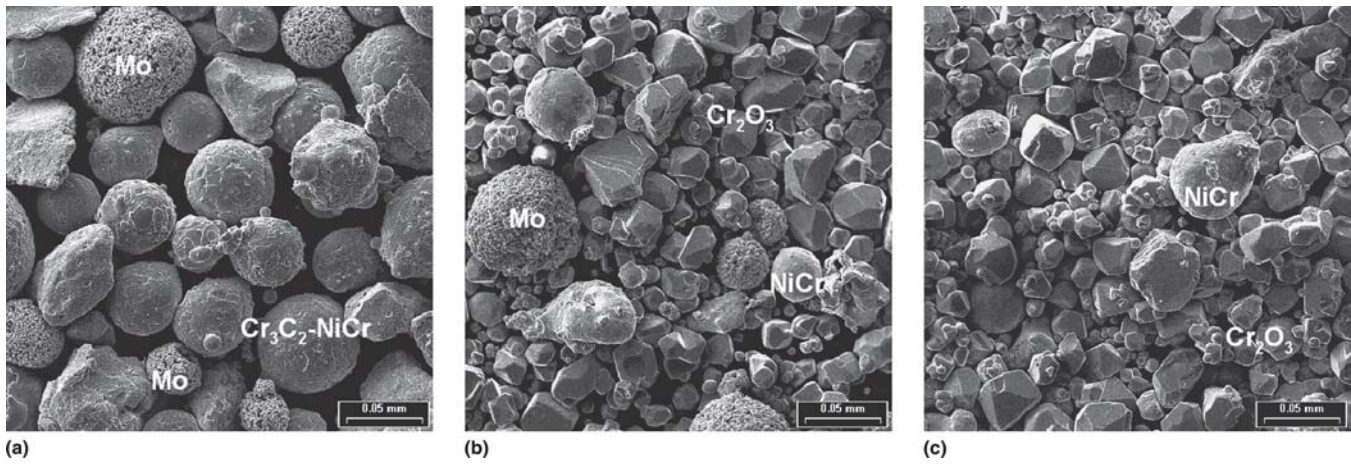


Fig. 1 Powder morphologies of the coating materials made for plasma spraying coating

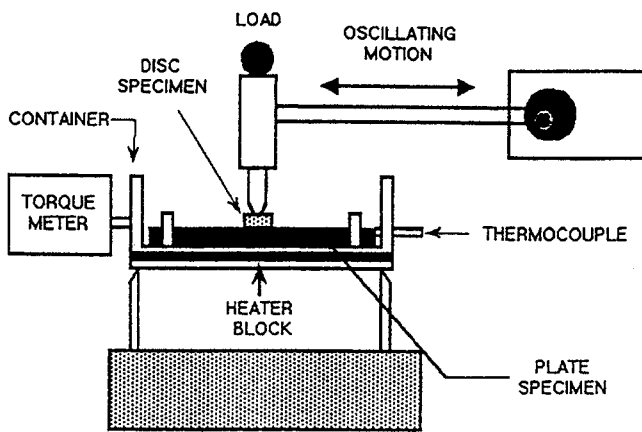


Fig. 2 Reciprocating disc-on-plate wear test machine used in this study

Table 2 Wear test map employed in this study

Wear test combinations		Disc, piston ring	
		Bare, CV cast iron	P2CM-coated
Plate, cylinder liner	Bare, gray cast iron	COM-1	COM-4
	P2ON-coated	COM-2	COM-5
	P3ONM-coated	COM-3	COM-6

with the highest hardness but lower porosity for field applications. To do this, the coating was accomplished on the gray and compact vermicular cast iron bulk. Materials used for coatings in this study are a  $\text{Cr}_2\text{O}_3$ -based and a  $\text{Cr}_3\text{C}_2$ -based coating with varying Mo content and were formulated by mixing of the feed stock powder materials. Properties and wear characteristics of the plasma spray coating were evaluated in terms of the porosity content and hardness level of the coated layer, friction coefficient, surface roughness, and mass change, respectively. On the basis of these analysis results, the optimum coating materials were suggested to improve wear life of both the piston ring and the cylinder liner.

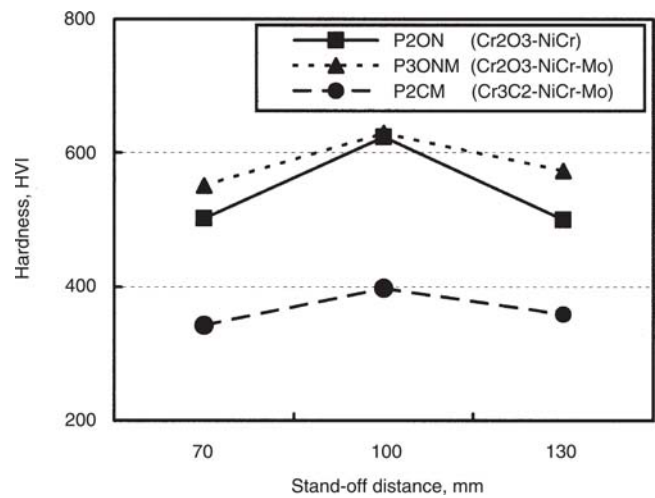


Fig. 3 Hardness variation of the coated layers as a function of stand-off distance (spraying conditions: arc current 500 A, voltage 70 V, traverse speed 50 m/min, powder feed rate 95 g/min)

## 2. Experimental Procedures

### 2.1 Substrates and Coating Materials

Base materials used in this study were a gray cast iron (230HB) and a compacted vermicular (CV) cast iron (250HB), which are used for cylinder liner and piston ring material, respectively. Cylinder liner material was machined to plate form ( $58 \times 38 \times 4$  mm) while piston ring material was made in a disc form ( $\varnothing 12 \times 4$  mm). Characteristics of four different coating source powders ( $\text{Cr}_3\text{C}_2$ -NiCr, Ni-Cr, Mo,  $\text{Cr}_2\text{O}_3$ ) used in this study are summarized in Table 1, and three coating materials were formulated using these powders: P2ON, P3ONM, and P2CM. P2ON and P3ONM are composed of Cr-oxide and NiCr powder in a ratio of 4:1 and Cr-oxide, NiCr, and Mo powder in a ratio of 4:1:1, respectively, while P2CM is composed of Cr-carbide, NiCr, and Mo powder in a ratio of 2:1:2. Figure 1 shows typical morphologies of the formulated coating materials.



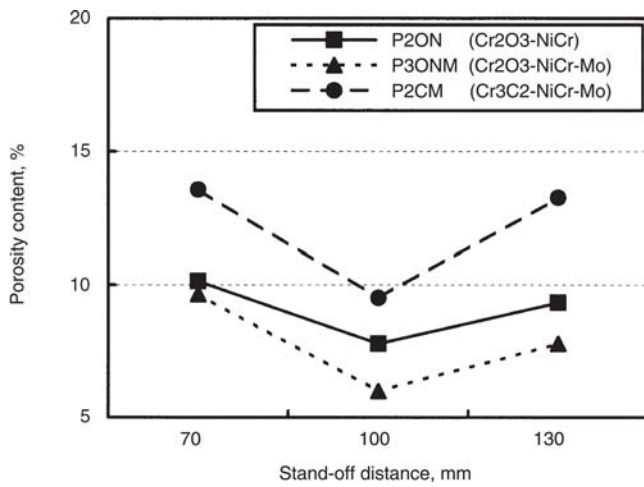


**Fig. 4** Porosity content variation of the coated layers as a function of stand-off distance (spraying conditions: arc current 500 A, voltage 70 V, traverse speed 50 m/min, powder feed rate 95 g/min)

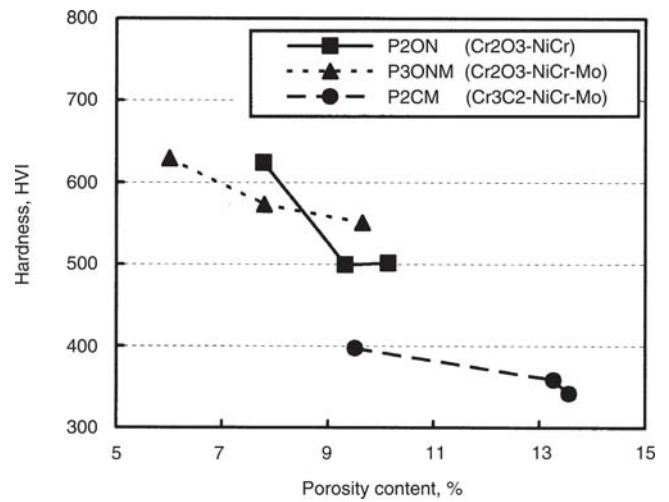


**Fig. 5** Relationship between porosity content and hardness of plasma sprayed coating layers (spraying conditions: arc current 500 A, voltage 70 V, traverse speed 50 m/min, powder feed rate 95 g/min)

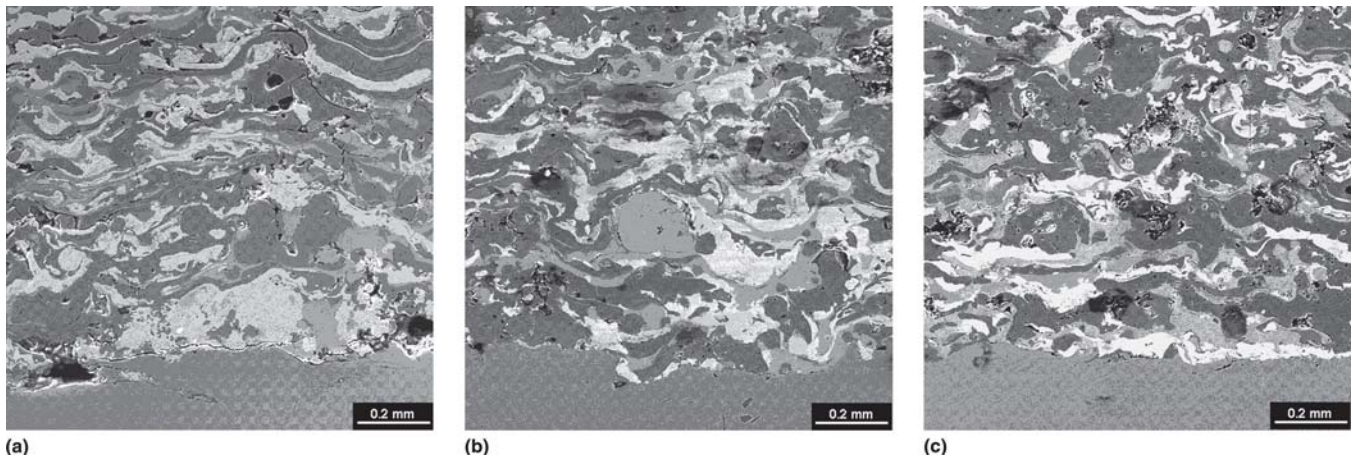


**Fig. 6** Typical microstructures of the P2CM-coated layers as a function of stand-off distance (spraying conditions: arc current 500 A, voltage 70 V, traverse speed 50 m/min, powder feed rate 95 g/min): (a) 70 mm, (b) 100 mm, (c) 130 mm

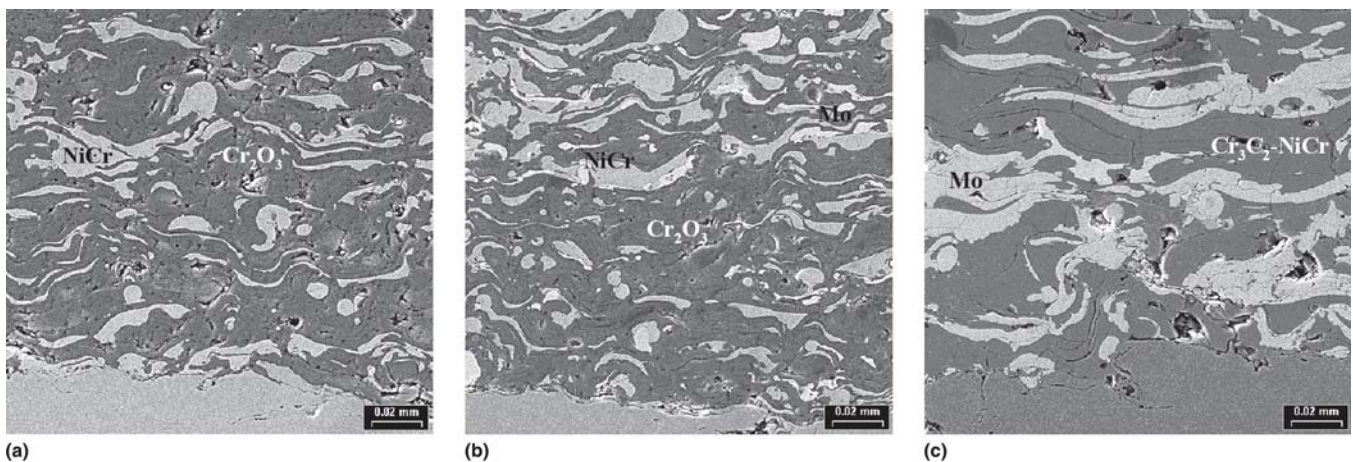


**Fig. 7** Typical microstructures of the coated layers formed at the optimum spraying condition selected within the window of this study (spraying conditions: arc current 500 A, voltage 70 V, traverse speed 50 m/min, powder feed rate 95 g/min, stand-off distance 100 mm): (a) P2ON, (b) P3ONM, (c) P2CM

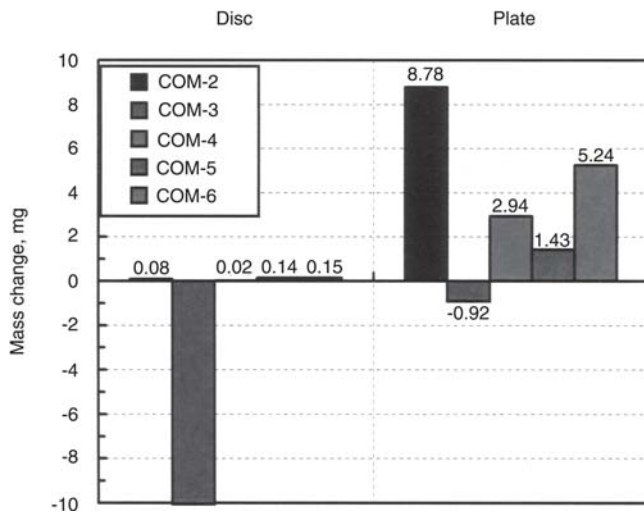


**Fig. 8** Mass change of disc and plate measured from each friction pair after wear test (wear test conditions: load 80 N, frequency 20 Hz, stroke 15 mm, temperature 450 °C without lubrication)

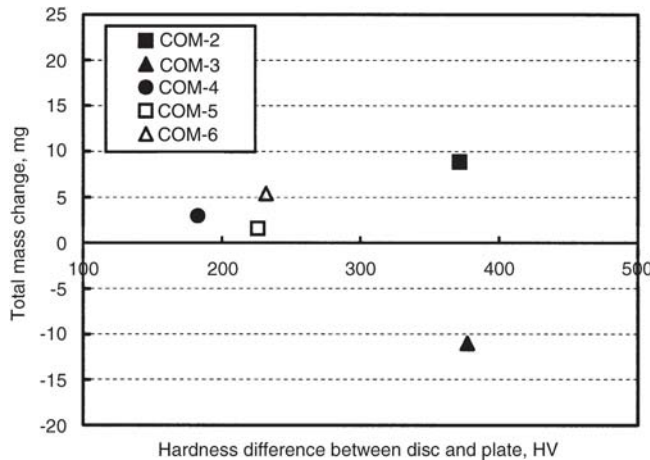


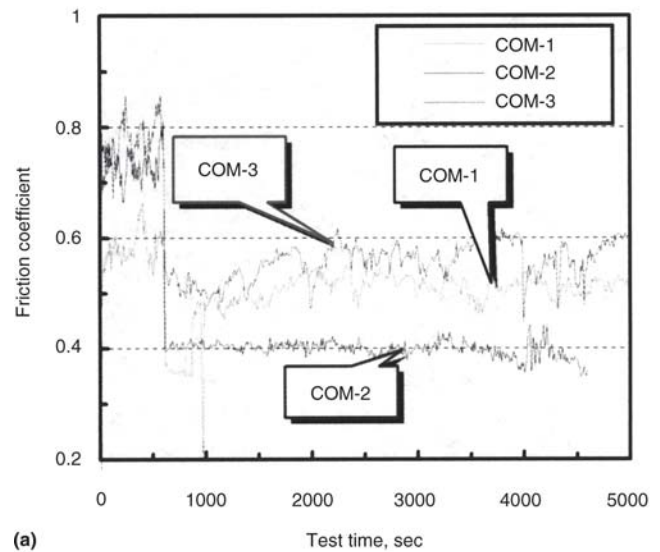
**Fig. 9** Total mass change of each friction pair as a function of the hardness difference between disc and plate after wear test (wear test conditions: load 80 N, frequency 20 Hz, stroke 15 mm, temperature 450 °C without lubrication)

**Table 3** Typical characteristics of the coated layers achieved at the optimum spraying condition selected within the framework of this study

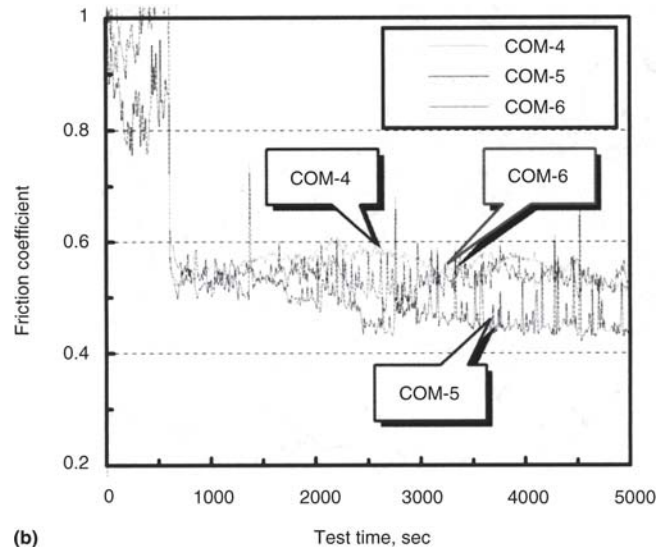
Designated name	Porosity content, %	Hardness, HV
P2ON	6.0-9.0	605-665
P3ONM	1.5-3.0	595-670
P2CM	9.0-10.0	375-420

## 2.2 Plasma Spray Coatings

Prior to coating, all substrates were prepared through the following procedures: (1) pickling and degreasing for removing surface organic matters; (2) cleaning in an ultrasonic bath; (3) blasting using aluminum oxide grit to enhance the binding strength between substrate and coating layer, and finally (4)



(a)



(b)

**Fig. 10** Friction coefficient variations of the designed friction pairs during wear test (wear test conditions: load 80 N, frequency 20 Hz, stroke 15 mm, temperature 450 °C without lubrication): (a) uncoated disc, (b) P2CM-coated disc

recleaning using acetone in an ultrasonic bath after removal of any remaining grit by compressed air. A preliminary test was conducted to optimize the plasma spray conditions. All the process parameters (e.g., arc current of 500 A and voltage of 70 V, specimen traverse speed of 50 m/min, powder feed rate of 95 g/min under an atmosphere of Ar/H<sub>2</sub> mixed gas) were maintained constant except for the stand-off distance, which varied from 70 to 130 mm. Each plasma-sprayed coating was made to a coating thickness of ~500 μm.

## 2.3 Wear Tests

Wear tests were carried out using an oscillating high-frequency friction machine according to ASTM G133 standard (Ref 9), as shown in Fig. 2. Wear tests were conducted under the condition of 80 N load, oscillating frequency of 20 Hz with stroke of 15 mm at temperature of 450 °C without lubrication by oscillating the disc specimen (∅ 12 × 4 mm, piston ring



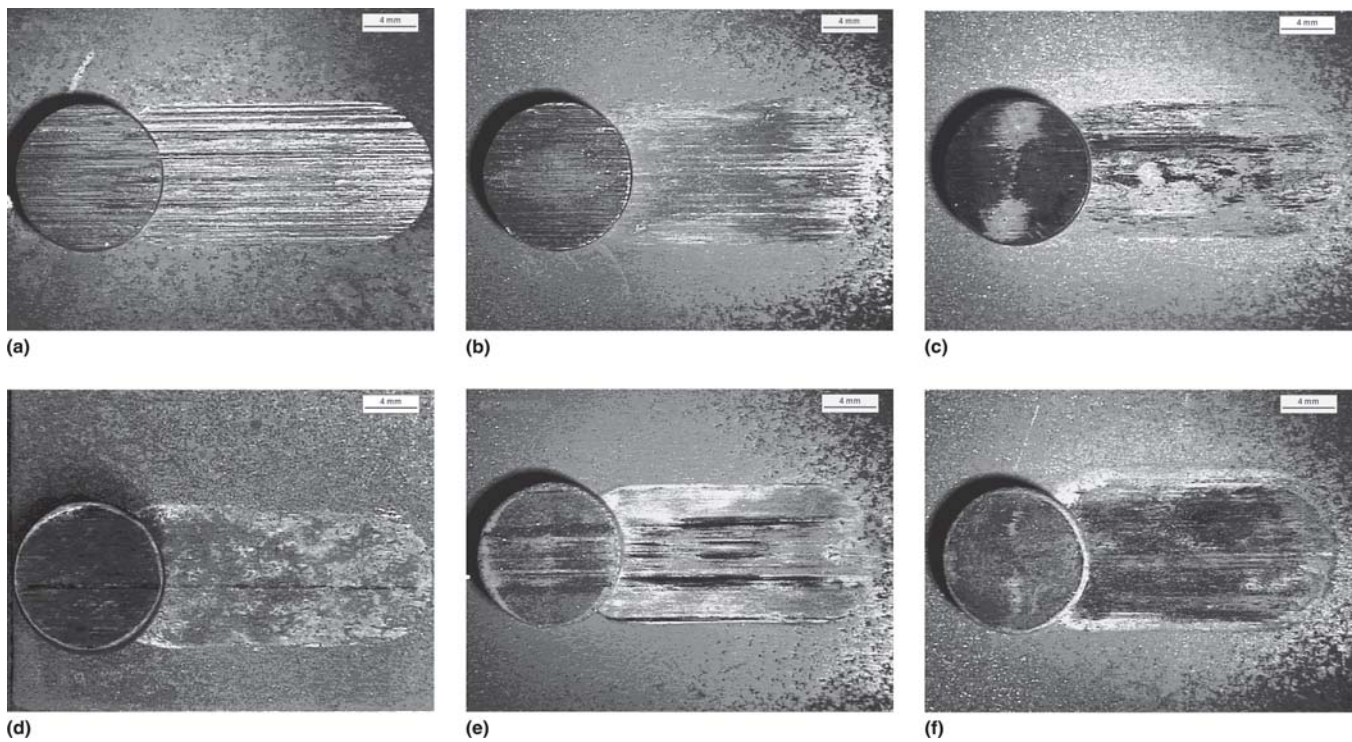


**Fig. 11** Macroviews of wear scars according to the friction pair after wear test (wear test conditions: load 80 N, frequency 20 Hz, stroke 15 mm, temperature 450 °C without lubrication): (a) COM-1, (b) COM-2, (c) COM-3, (d) COM-4, (e) COM-5, (f) COM-6

material) against the stationary plate specimen (58 × 38 × 4 mm, cylinder liner material) to simulate the reciprocating motion between the piston ring and cylinder liner of the actual engine system. Prior to wear testing, all of the specimens were polished with Emery paper (#400) to give the same surface conditions. All of the test runs were conducted for 1.5 h after run-in for 10 min at the wear test condition mentioned above. To study the effect of the coating materials on the wear characteristics, six combinations of friction pairs were tested as shown in Table 2. For example, COM-5 means a friction pair that consists of a plate coated with Cr<sub>2</sub>O<sub>3</sub>-NiCr and a disc coated with Cr<sub>3</sub>C<sub>2</sub>-NiCr-Mo.

#### 2.4 Evaluations of Wear Characteristics

Surface roughness of all the specimens was evaluated before/after wear test in terms of arithmetic average value ( $R_a$ ) by a stylus-type roughness tester. Mass change was measured using an automatic mass balance with an accuracy of 10<sup>-4</sup> g. To investigate the wear characteristics, such as wear pattern and surface morphology, both topo- and metallographic observations on the worn surface of the coated layer were carried out using a scanning electron microscope (SEM) and an optical microscope (OM).

### 3. Results and Discussion

#### 3.1 Optimization of Plasma Spray-Coated Quality

Wear life of the coated system strongly depends on the characteristics of the coating layer, i.e., bonding strength between splats, homogeneity, porosity content, and hardness level of the coated layer. Figure 3 shows the hardness varia-

tions of the coated layers as a function of stand-off distance. The maximum hardness value is achieved at 100 mm stand-off distance regardless of coating materials used, and the Cr<sub>2</sub>O<sub>3</sub>-NiCr-Mo-coated layer shows a higher hardness level than others regardless of the stand-off distance. Meanwhile, the minimum porosity content is also obtained at 100 mm stand-off distance and Cr<sub>2</sub>O<sub>3</sub>-NiCr-Mo-coated layer shows the lowest level throughout all the stand-off distances studied as shown in Fig. 4. As a result, it is found that hardness levels of the plasma spray-coated layer depends on the porosity content as well as the coating materials used, as shown in Fig. 5. Porosity content of the coated layer is greatly affected by the spraying condition. For instance, it can be found there are big differences in porosity and crack content between three conditions from Fig. 6 showing typical microstructures of the Cr<sub>3</sub>C<sub>2</sub>-NiCr-Mo-coated layers as a function of stand-off distance. These differences in porosity and crack content can be explained by the combined effect of both the coating powder's melting state that varies during its voyage and shrinkage amount and wet-ability of the spraying powder occurring during its collision onto substrate and/or coating layer. For shorter stand-off distance (at 70 mm), the shrinkage amount is larger due to a higher solidifying temperature than a longer distance, whereas for a longer stand-off distance (at 130 mm) the wettability becomes weak because the powder's surface has already solidified somewhat due to a temperature drop during its voyage. From these results, the porosity and crack content appear to be greatly affected by both stand-off distance and properties of the coating material used. The characteristics of the coated layers achieved at the optimum spray condition that maximizes hardness but minimizes the porosity content of coated layer are summarized in Table 3.

Figure 7 exhibits typical microstructures of the coated lay-



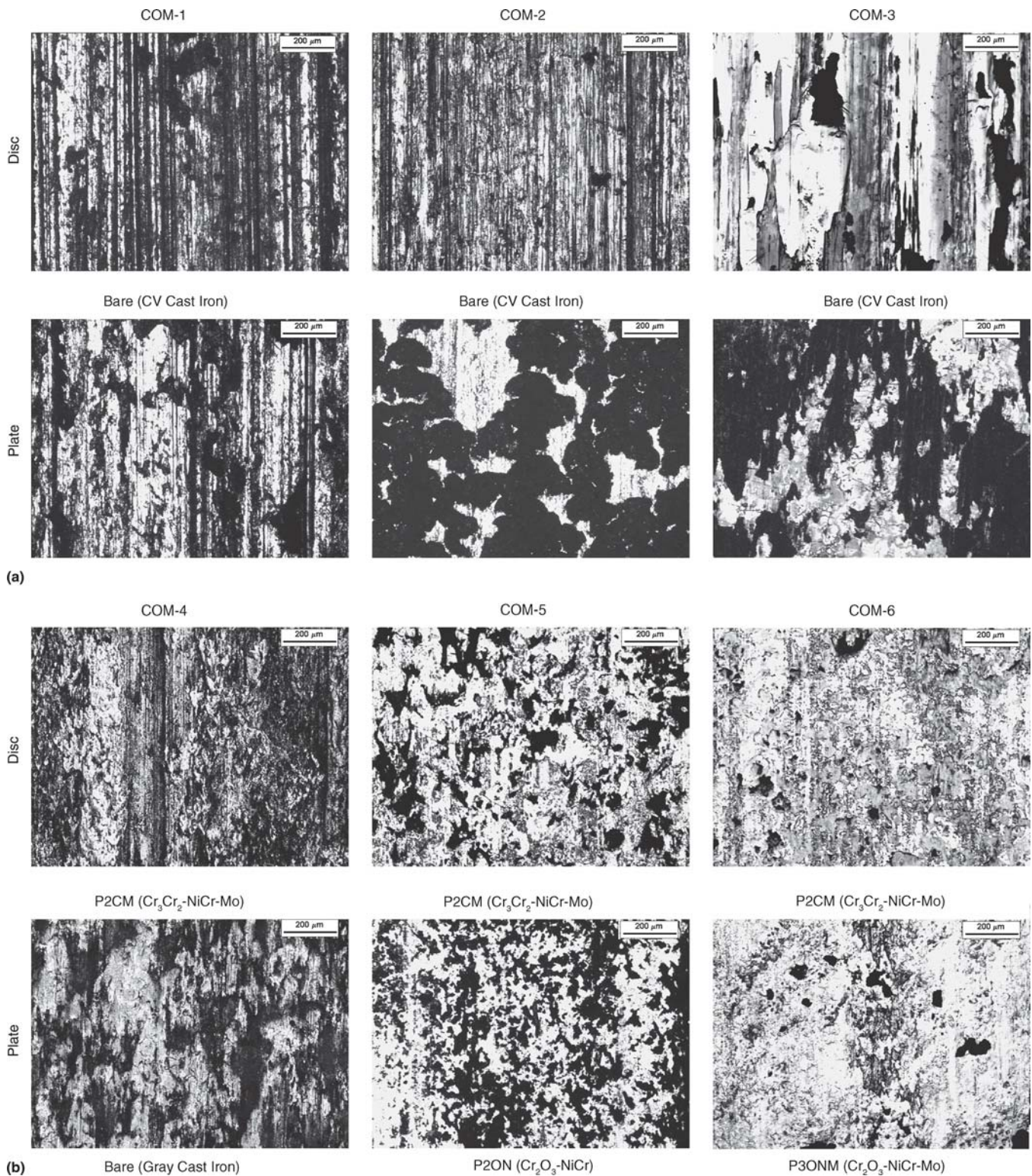


**Fig. 12** Microviews of wear scars according to the friction pair after wear test (wear test conditions: load 80 N, frequency 20 Hz, stroke 15 mm, temperature 450 °C without lubrication): (a) uncoated disc; (b) P2CM-coated disc

ers formed at the optimum spraying condition selected within the scope of this study. There are apparent differences in their morphologies, e.g., splat sizes and shapes. The microstructure of a P2ON-coated layer consists of a dark phase of Cr<sub>2</sub>O<sub>3</sub> splats and a gray phase of NiCr splats; P3ONM has a white phase of Mo, a gray phase of NiCr, and a dark phase of Cr<sub>2</sub>O<sub>3</sub>; and

P2CM has a white phase of Mo and a gray phase of Cr<sub>3</sub>C<sub>2</sub>-NiCr. Of these three coating layers, P2CM has the largest splat size. This is, of course, due to the use of a larger powder size than others, as shown in Fig. 1. From Fig. 5, which indicates the porosity content and hardness level of the coating layer, it can be seen that the P3ONM contains a relatively lower amount

of porosity, consequently possessing higher hardness. These differences in porosity content and hardness level of the coated layers are generally related to the chemical and physical characteristics of the powders used.

### 3.2 Wear Characteristics

Figure 8 shows the mass change of disc and plate measured from each friction pair after wear testing. Most plates gained a mass, whereas the mass change of the discs showed very similar patterns except with COM-3. It is believed that the mass increases by the transfer of material from the mating surface, possibly including wear debris and some oxide formed at higher friction temperature (Ref 10). COM-5 ( $\text{Cr}_3\text{C}_2$ -NiCr-Mo-coated piston ring/ $\text{Cr}_2\text{O}_3$ -NiCr-coated cylinder liner) shows the best wear life in terms of total mass change. The magnitude of total mass change increases with an increase of the hardness difference between mating specimens, as shown in Fig. 9, indicating the total mass change of each friction pair according to the hardness difference between disc and plate after wear testing. Therefore, it is effective to minimize the hardness difference between the mating pairs for improving wear life of the system. Figure 10 displays the friction coefficient variation of the designed friction pairs with operating times during wear testing. Among the tests with uncoated discs (COM-1, -2, and -3), COM-2 revealed the lowest mean friction coefficient value,  $\sim 0.4$ , but among the tests with the P2CM-coated discs (COM-4, -5, and -6), COM-5 has the lowest value. It is generally known that the friction coefficient depends on both the coating materials' properties and their wear mechanism occurring during wear test. Figures 11 and 12 show macro- and microviews of wear scars according to the friction pairs after wear testing. COM-1 and -2 make a lot of scratches on "both" worn surfaces, but the COM-1 friction pair that was tested with a bare disc on bare plate shows deeper and wider scratches. Scratches are caused mainly by abrasive wear mechanisms, which suggests that wear of the component should occur by introduction of foreign particles separated from the worn-out material itself during wear test. On the other hand, for P2CM-coated "discs" (COM-4, -5, and -6), all of the wear tracks for both discs and plates show relatively smooth surfaces with few scratches. These smooth surfaces are produced mainly by adhesive wear mechanisms, implying the friction progressed by direct metal contact between the disc and the plate without intermediate particles. It has been reported that the formation of a smooth layer, like these patterns in the plasma-sprayed coating, is related to material transfer as well as to deformation of the surface layer during wear testing (Ref 8). Generally, the morphology and roughness of the worn surface formed after wear testing are determined by the main wear mechanism actions. Figure 13 shows surface roughness measured from wear scars of disc and plate after the wear test. COM-1 indicates a much higher roughness value than the other coated one in both disc and plate specimens. For example, roughness of the disc in COM-1 is about  $5.4 \mu\text{m}$  in  $R_a$ , whereas other coated discs ranged from  $0.4$  to  $2.0 \mu\text{m}$  in  $R_a$ . An increase in surface roughness of COM-1 friction pair was attributed to an increase in the wear rate caused by its lower hardness in comparison with the other coated one. Among the friction pairs with one side and both sides with coated layers (COM-2, -3, -4, -5, and -6), COM-6 shows the lowest surface roughness level in both of their worn surfaces.

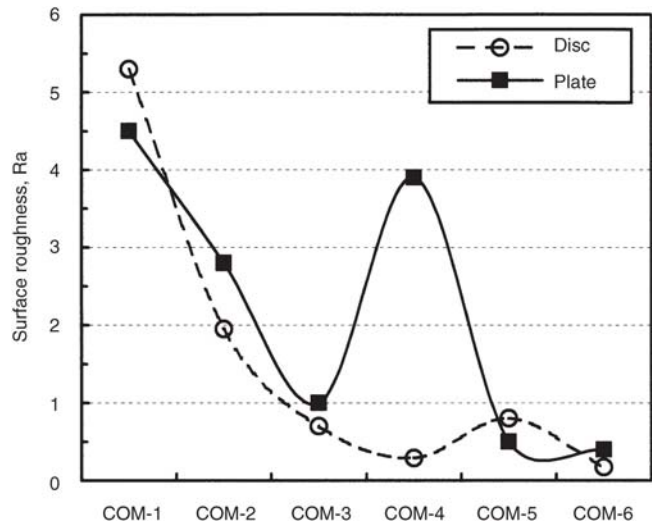


Fig. 13 Surface roughness values of disc and plate according to the friction pair after wear test (wear test conditions: load 80 N, frequency 20 Hz, stroke 15 mm, temperature  $450^\circ\text{C}$  without lubrication)

Table 4 Mean friction coefficients and surface roughness values obtained from each friction pair after wear test

Combinations of friction pair, disc plate	Mean friction coefficient, $\mu$	Surface roughness, $\mu\text{m}$	
		Disc	Plate
COM-1 (CV cast iron/gray cast iron)	0.501	$R_a$ 5.30 $R_{max}$ 30.4	$R_a$ 4.50 $R_{max}$ 39.2
COM-2 (CV cast iron/ $\text{Cr}_2\text{O}_3$ -NiCr)	0.398	$R_a$ 1.95 $R_{max}$ 12.0	$R_a$ 2.80 $R_{max}$ 30.8
COM-3 (CV cast iron/ $\text{Cr}_2\text{O}_3$ -NiCr-Mo)	0.566	$R_a$ 0.70 $R_{max}$ 9.10	$R_a$ 1.00 $R_{max}$ 11.2
COM-4 (commercial design) ( $\text{Cr}_3\text{C}_2$ -NiCr-Mo/gray cast iron)	0.555	$R_a$ 0.30 $R_{max}$ 3.10	$R_a$ 3.90 $R_{max}$ 30.8
COM-5 ( $\text{Cr}_3\text{C}_2$ -NiCr-Mo/ $\text{Cr}_2\text{O}_3$ -NiCr)	0.479	$R_a$ 0.80 $R_{max}$ 12.8	$R_a$ 0.50 $R_{max}$ 14.4
COM-6 ( $\text{Cr}_3\text{C}_2$ -NiCr-Mo/ $\text{Cr}_2\text{O}_3$ -NiCr-Mo)	0.536	$R_a$ 0.17 $R_{max}$ 6.30	$R_a$ 0.40 $R_{max}$ 6.60

Wear test conditions: load, 80 N; frequency, 20 Hz; stroke, 15 mm; temperature  $450^\circ\text{C}$ ; no lubrication

Table 4 summarizes the mean friction coefficients and surface roughness values obtained from each friction pair after wear testing. Among six materials combinations, the friction pairs bearing molybdenum powder in the coated layers (that is, COM-3, -4, -5, and -6) showed somewhat higher friction coefficients but lower surface roughness. It is well known that molybdenum is an element added that can improve the high-temperature fracture toughness without sacrificing the wear properties (Ref 11), which in turn generally contributes to improving wear resistance by decreasing the break-away amount of the coating particle because of its role as a solid lubricant. But molybdenum-base coatings also give high friction coefficients (Ref 12). This may be caused by adhesive wear mechanisms. Generally, adhesive friction has a larger total contact area than abrasive friction during a wear test; thus it is natural that the friction coefficient value would be increased. The difference between COM-5 and COM-6 is a good example. The



friction pair of COM-5 ( $\text{Cr}_2\text{O}_3$ -NiCr-coated cylinder liner against  $\text{Cr}_3\text{C}_2$ -NiCr-Mo-coated piston ring) shows a lower friction coefficient but a higher surface roughness than the combination of COM-6 ( $\text{Cr}_2\text{O}_3$ -NiCr-Mo-coated cylinder liner against  $\text{Cr}_3\text{C}_2$ -NiCr-Mo-coated piston ring). However, any combination of these two cases has a lower friction coefficient and lower surface roughness than the commercially applied combination (COM-4). Consequently, it is beneficial to coat both mating surfaces to achieve better wear resistance properties.

#### 4. Conclusions

From a study of the wear characteristics of several friction pairs between plasma spray coating the piston ring and cylinder liner as a function of the coating materials to find an optimum combination of coating materials using the disc-on-plate reciprocating wear test, the following conclusions can be drawn.

- It was found that a dissimilar coating combination of  $\text{Cr}_2\text{C}_3$ -NiCr-Mo for the piston ring and  $\text{Cr}_2\text{O}_3$ -NiCr-Mo for the cylinder liner would provide the best antiwear performance.
- It was also found that molybdenum was beneficial to improve wear characteristics of the coating.
- Hardness differences between mating surfaces were found to be wear-determining factors that should be controlled below 300 (in Vickers hardness scale) under dry conditions.
- Adhesive wear accompanied by metal transfer was a dominant wear mechanism under unlubricated conditions for the materials systems studied.

#### References

1. S. Mitsutake, S. Ono, K. Maekawa, F. Takahashi, and A. Deguchi, Lubrication of Cylinder Liners and Piston Rings of Low-Speed Marine Diesel Engines, *Mitsubishi Tech. Rev.*, 1987, **24**(2), p 87-93
2. C. Schenk, J. Hengeveld, and K. Aabo, The Role of Temperature and Pressure in Wear Processes in Low Speed Diesel Engines, *Proc. 6th Int. Symp. Marine Engineering* (Tokyo, Japan), October 23-27, 2000
3. M.G.S. Naylor and M.P. Fear, "Development of Wear-Resistant Ceramic Coatings for In-Cylinder Diesel Engine Components," Presented at the *Coatings for Advanced Heat Engines Workshop* (Castine, Maine), August 6-9, 1990
4. F.G. Cantow, Piston Rings for High Output 4 Stroke Diesel Engines, *Proc. 6th Int. Symp. on Marine Engineering* (Tokyo, Japan), October 23-27, 2000, p 973-980
5. S. Miyake, T. Tanaka, T. Goto, and T.S. Knudsen, Development of Spray-Coated Cylinder Liner for Marine Engine, *Proc. CIMAC Congress* (Hamburg, Germany), 2001, p 913-920
6. P. Sahoo, High-Performance Wear Coatings—The Quest Continues, *Powder Metall. Int.*, 1993, **25**(2), p 73-78
7. Y. Kitajima, Application of Wear Resistance Spraying for Diesel Engine, *J. Jpn. Therm. Spray. Soc.*, 1999, **36**(1), p 46-51
8. M. Tanaka, Y. Kitajima, Y. Endoh, M. Watanabe, and Y. Nagita, Ceramic-Metal Composite Coated Piston Ring and Cylinder Liner of Marine Low Speed Diesel Engine, *J. Mar. Eng. Soc. Jpn.*, 1992, **27**(3), p 238-247
9. A.G. Plint and M.A. Plint, A New Technique for the Investigation of Stick-Slip, *Tribol. Int.*, 1985, **18**, p 247-249
10. H.S. Ahn and O.K. Kwan, Tribological Behaviour of Plasma-Sprayed Chromium Oxide Coatings, *Wear*, 1999, **225-229**, p 814-824
11. F. Rastegar and D.E. Richardson, Alternative to Chrome: HVOF Cermet Coatings for High Horse Power Diesel Engines, *Surf. Coat. Technol.*, 1997, **90**, p 156-163
12. M.G.S. Naylor and M.P. Fear, "Development of Wear-Resistant Ceramic Coatings for In-Cylinder Diesel Engine Components," Paper presented at the *Coatings for Advanced Heat Engines Workshop* August 6-9 (Castine, Maine), 1990